Off-resonant quantum Zeno and anti-Zeno effects on entanglement

2010 Phys. Scr. 2010 014044

(http://iopscience.iop.org/1402-4896/2010/T140/014044)

Phys. Scr. **T140** (2010) 014044 (5pp) doi:10.1088/0031-8949/2010/T140/014044

Off-resonant quantum Zeno and anti-Zeno effects on entanglement

F Francica[1], S Maniscalco[2] and F Plastina[1]

[1] Dipartimento di Fisica, Università della Calabria and INFN—Gruppo collegato di Cosenza, 87036 Arcavacata di Rende (CS), Italy
[2] Turku Centre for Quantum Physics, Department of Physics and Astronomy, University of Turku, FIN-20014 Turku, Finland

E-mail: francica@fis.unical.it

Received 29 March 2010
Accepted for publication 16 June 2010
Published 30 September 2010
Online at stacks.iop.org/PhysScr/T140/014044

Abstract
We examine the appearance of Zeno and anti-Zeno effects (Misra and Sudarshan 1977 *J. Math. Phys.* **18** 756; Kofman and Kurizki 2000 *Nature* **405** 546; Kofman and Kurizki 1996 *Phys. Rev.* A **54** 3750; Facchi *et al* 2001 *Phys. Rev. Lett.* **86** 2699) in the entanglement dynamics of two qubits off-resonantly coupled to the same lossy cavity when the unitary evolution of the system is interrupted by repeated projective measurements. We describe in detail these quantum effects by comparing the measurement-induced coarse-grained dynamics to the entanglement evolution in the absence of measurements in several scenarios (Francica *et al* 2009 *Phys. Rev.* A **79** 032310). In particular, we examine the strong and weak coupling regimes, the role of the relative coupling strengths between the two qubits and the reservoir and the effect of the detuning from the main cavity frequency. We show that the anti-Zeno effect can occur in the entanglement dynamics when the qubit frequencies are detuned from the main reservoir frequency. Furthermore, we find that Zeno and anti-Zeno effects can even appear sequentially many times as a function of the interval between the measurements. Finally, we show that, in the off-resonant regime, we can preserve the entanglement using the quantum Zeno effect more efficiently than in the resonant limit (Maniscalco *et al* 2008 *Phys. Rev. Lett.* **100** 090503), even if, in this case, no sub-radiant state exists.

PACS numbers: 42.50.Ct, 42.50.Ar, 42.50.Dv

(Some figures in this article are in colour only in the electronic version.)

1. Introduction

The effects of very frequent measurements on the decay rate of any unstable quantum state have been widely discussed in both theoretical [5] and, more recently, experimental works [6]. It was found that frequent measurements can reduce or accelerate the decay process: these are the quantum Zeno and anti-Zeno effects, respectively [1, 10].

In this paper, we investigate the entanglement dynamics of two qubits off-resonantly coupled to a common reservoir, in the presence of measurements. We show that the quantum Zeno and anti-Zeno effects on entanglement [3, 11] stem from the competing action of the off-resonant interaction and of the repeated projective measurements. Moreover, when the measurement time interval approaches zero, the quantum Zeno effect dominates the dynamics in the far off-resonant limit, whereas for greater values of the measurement time interval, the quantum anti-Zeno effect can appear, reducing the capability of the system to store entanglement.

We consider the following Hamiltonian describing an open quantum system consisting of two qubits coupled to a common zero-temperature bosonic reservoir in the vacuum:

$$H = H_S + H_R + H_{int}, \tag{1}$$

where H_S is the Hamiltonian of the qubits coupled, via the interaction Hamiltonian H_{int}, to the common reservoir, and H_R is the reservoir Hamiltonian.

The Hamiltonian for the total system, in the dipole and the rotating-wave approximations, and in units of $\hbar = 1$, can be written as

$$H_S = \omega_1 \sigma_+^{(1)} \sigma_-^{(1)} + \omega_2 \sigma_+^{(2)} \sigma_-^{(2)}, \quad (2)$$

$$H_R = \sum_k \omega_k b_k^\dagger b_k, \quad (3)$$

$$H_{\mathrm{int}} = \left(\alpha_1 \sigma_+^{(1)} + \alpha_2 \sigma_+^{(2)}\right) \sum_k g_k b_k + \mathrm{h.c.}, \quad (4)$$

where $b_k^\dagger$ and b_k are the creation and annihilation operators of quanta of the reservoir, $\sigma_\pm^{(j)}$ and ω_j are the inversion operators and the transition frequency of the jth qubit ($j = 1, 2$), respectively, ω_k is the frequency of the reservoir kth mode and $\alpha_j g_k$ describes the coupling strength between the jth qubit and the kth mode of the reservoir.

Here, α_j are dimensionless real coupling constants measuring the interaction strength of each single qubit with the reservoir. In the case of two atoms inside a cavity, e.g. different values of α_j can be obtained by changing the relative position of the atoms in the cavity field standing wave. We denote with $\alpha_T = (\alpha_1^2 + \alpha_2^2)^{1/2}$ the collective coupling constant and with $r_j = \alpha_j / \alpha_T$ the relative interaction strength.

We restrict ourselves to the case in which only one excitation is present in the system and the reservoir is in a vacuum. We consider the initial state

$$|\Psi(0)\rangle = [c_{01}\,|1\rangle_1\,|0\rangle_2 + c_{02}\,|0\rangle_1\,|1\rangle_2] \bigotimes_k |0_k\rangle_R\,, \quad (5)$$

where c_{01} and c_{02} are complex numbers, $|0\rangle_j$ and $|1\rangle_j$ ($j = 1, 2$) are the ground and excited states of the jth qubit, respectively, and $|0_k\rangle_R$ is the state of the reservoir with zero excitations in the kth mode.

The time evolution of the total system is given by

$$|\Psi(t)\rangle = c_1(t)|1\rangle_1|0\rangle_2|0\rangle_R + c_2(t)|0\rangle_1|1\rangle_2|0\rangle_R + \sum_k c_k(t)|0\rangle_1|0\rangle_2|1_k\rangle_R, \quad (6)$$

with $|1_k\rangle_R$ being the state of the reservoir with only one excitation in the kth mode.

In the standard basis, the reduced density matrix, obtained from the density operator $|\Psi(t)\rangle\langle\Psi(t)|$ after tracing over the reservoir degrees of freedom, takes the form

$$\rho(t) = \begin{pmatrix} 0 & 0 & 0 & 0 \\ 0 & |c_1(t)|^2 & c_1(t)c_2^*(t) & 0 \\ 0 & c_1^*(t)c_2(t) & |c_2(t)|^2 & 0 \\ 0 & 0 & 0 & 1 - |c_1|^2 - |c_2|^2 \end{pmatrix}. \quad (7)$$

The two-qubit dynamics is therefore completely characterized by the amplitudes $c_{1,2}(t)$. For certain specific structures of the reservoir, one can obtain the exact analytical expressions of $c_{1,2}(t)$ by the Laplace transform method. In this paper, we consider a structured reservoir describing the electromagnetic field inside a lossy cavity. This case can be modelled by a Lorentian broadening of the fundamental mode cavity. In [2], we have found the exact, and therefore non-Markovian, analytical expression for the amplitudes $c_{1,2}(t)$.

2. Observed entanglement dynamics

The entanglement dynamics for a generic initial two-qubit state containing one excitation coupled to a common structured reservoir was investigated in [2, 3]. We choose the concurrence $\mathcal{C}(t)$ [4], ranging from 0 for separable states to 1 for maximally entangled states, to quantify the amount of entanglement encoded into the two-qubit system. The explicit analytic expression of $\mathcal{C}(t)$ can be obtained from the reduced density matrix of equation (7). It is easy to show that the concurrence takes a very simple form

$$\mathcal{C}(t) = 2\,|c_1(t)|\;|c_2(t)|\,. \quad (8)$$

In [3], we have shown how, in the resonant regime, repeated non-selective measurements on the collective qubits system induce the quantum Zeno effect on entanglement and we have proven that, in this way, one can achieve efficient entanglement protection. In the following, we analyse the effect of measurements on the entanglement dynamics in the off-resonance regime. In particular we will demonstrate the occurrence of both quantum Zeno and anti-Zeno effects on entanglement, depending on the measurement time interval.

We recall that, in order to observe the quantum Zeno effect on entanglement, the series of non-selective measurements on the collective atomic system, performed at time intervals T, must have the following two properties: (i) one of the possible measurement outcomes is the projection onto the collective ground state $|\psi_0\rangle = |0\rangle_1|0\rangle_2$ and (ii) the measurement cannot distinguish between the excited states $|\psi_1\rangle = |1\rangle_1|0\rangle_2$ and $|\psi_2\rangle = |0\rangle_1|1\rangle_2$.

Such measurements are described by the following two projectors:

$$\Pi_0 = |\psi_0\rangle\,\langle\psi_0| \otimes I_R, \quad (9)$$

$$\Pi_1 = (|\psi_-\rangle\,\langle\psi_-| + |\psi_+\rangle\,\langle\psi_+|) \otimes I_R, \quad (10)$$

with I_R being the reservoir identity matrix. The action of the above operators is to project the qubits into the subspace S_1 spanned by

$$|\psi_-\rangle = r_2\,|1\rangle_1\,|0\rangle_2 - r_1\,|0\rangle_1\,|1\rangle_2\,,$$

$$|\psi_+\rangle = r_1\,|1\rangle_1\,|0\rangle_2 + r_2\,|0\rangle_1\,|1\rangle_2\,.$$

We note that, for $\omega_1 = \omega_2$, the above two states coincide with the subradiant and the superradiant state, respectively. Projective measurements as those described by the operator Π_0 can be implemented in both cavity quantum electrodynamics (QED) [7] and in superconducting circuits with on-chip qubits and resonator [8, 9].

Recasting the initial state in the form $|\psi(0)\rangle = \beta_-|\psi_-\rangle + \beta_+|\psi_+\rangle$, we can write the total state at time $t = NT$, i.e. after N measurements of the collective qubits system, as follows:

$$|\Psi^{(N)}(t)\rangle = \Pi_1|\Psi^{(N-1)}(t)\rangle = [\beta_-^{(N)}(T)\,|\psi_-\rangle + \beta_+^{(N)}(T)\,|\psi_+\rangle] \bigotimes_k |0_k\rangle_R, \quad (11)$$

where T is the time interval between two consecutive measurements and $\beta_\pm^{(N)}(T)$ are the survival amplitudes at

$t = NT$ in the presence of N measurements. The survival amplitudes can be expressed in terms of the initial amplitudes as follows:

$$\begin{pmatrix} \beta_+^{(N)}(T) \\ \beta_-^{(N)}(T) \end{pmatrix} = \mathbf{E}^N \begin{pmatrix} \beta_+ \\ \beta_- \end{pmatrix}, \qquad (12)$$

with

$$\beta_+ = r_1\, c_{10} + r_2\, c_{20}, \quad \beta_- = r_2\, c_{10} - r_1\, c_{20}. \qquad (13)$$

We characterize the initial state of the qubits in terms of the initial separability s defined via the equations

$$c_{10} = \sqrt{\frac{1-s}{2}}, \quad c_{20} = \sqrt{\frac{1+s}{2}}\, \mathrm{e}^{\mathrm{i}\phi}. \qquad (14)$$

One can see immediately that $s = \pm 1$ corresponds to a separable state, while $s = 0$ corresponds to a maximally entangled state.

In general, the explicit analytic expressions of the survivor amplitudes $\beta_\pm^{(N)}(T)$ are very complicated and do not provide a simple physical understanding. Nevertheless, one can always calculate the evolution matrix $\mathbf{E}^N$ iteratively.

For $\omega_1 = \omega_2$, a subradiant decoherence-free state $|\psi_-\rangle$ exists. This state does not evolve in time, so the only relevant time evolution is the one of the superradiant state $|\psi_+\rangle$. In this case the explicit expression for the survival amplitudes in the presence of measurements takes the simple form

$$\beta_-^{(N)}(T) = \beta_-, \quad \beta_+^{(N)}(T) = \mathcal{E}^N(T)\, \beta_+, \qquad (15)$$

with

$$\mathcal{E}(T) = \mathrm{e}^{-(\lambda - \mathrm{i}\delta)\, T/2} \left[\cosh\left(\frac{\Omega T}{2}\right) + \frac{\lambda - \mathrm{i}\delta}{\Omega} \sinh\left(\frac{\Omega T}{2}\right) \right], \qquad (16)$$

where $\delta_1 = \delta_2 \equiv \delta$ and $\Omega = \sqrt{\lambda^2 - \Omega_R^2 - \mathrm{i}2\delta\lambda}$. We denote by $\Omega_R = \sqrt{4W^2\alpha_T^2 + \delta^2}$ the generalized Rabi frequency and by $\mathcal{R} = W\alpha_T$ the vacuum Rabi frequency. The function $\mathcal{E}(T)$ is the survival amplitude of the superradiant state $\langle\psi_+(T)|\psi_+(0)\rangle = \mathcal{E}(T)$.

The entanglement of the observed two-qubit system, at time $t = NT$, can be evaluated by the concurrence $\mathcal{C}^{(N)}(t)$ in the presence of N measurements. This quantity is derived from the reduced density matrix describing the system observed N times, obtained from $|\Psi^{(N)}(t)\rangle\langle\Psi^{(N)}(t)|$ by tracing over the reservoir degrees of freedom. $\mathcal{C}^{(N)}(t)$, in the subradiant scenario ($\omega_1 = \omega_2$), can be written as

$$\mathcal{C}^{(N)}(t) = 2\Big| \left(r_1\beta_+\, \mathrm{e}^{\mathrm{i}\eta(T)t}\, \mathrm{e}^{-\gamma(T)t/2} + r_2\beta_-\right) \times \left(r_2\beta_+^*\, \mathrm{e}^{-\mathrm{i}\eta(T)t}\, \mathrm{e}^{-\gamma(T)t/2} - r_1\beta_-^*\right) \Big|, \qquad (17)$$

where

$$\gamma(T) = -\frac{\log\left[|\mathcal{E}(T)|^2\right]}{T}, \quad \eta(T) = \frac{\arg\left[\mathcal{E}(T)\right]}{T} \qquad (18)$$

are the effective decay rate and the argument of an oscillatory term, respectively.

We note that the dynamics of the concurrence in the presence of measurements can be expressed in a simple way in terms of the survival amplitudes $\beta_\pm^{(N)}(T)$ and therefore depends on T, on the 'position' of the Bohr frequencies of the atoms with respect to the spectrum, on the relative coupling between the qubits and the reservoir and on the quality factor of the cavity.

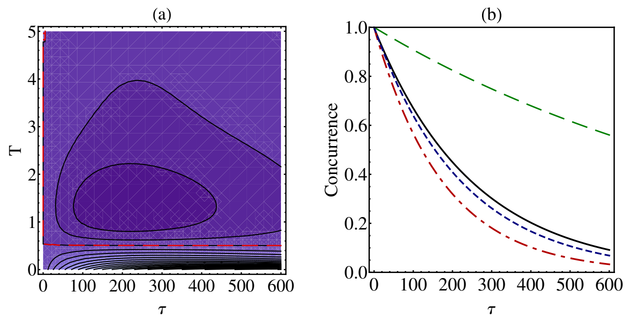

Figure 1. In the subradiant scenario ($\delta_1 = \delta_2$) and bad cavity limit ($R = 0.1$), for $s = 0$, $\delta = 2$ and $r_1 = 1/\sqrt{2}$: (a) contour plot of $\mathcal{C}^{(N)}(\tau) - \mathcal{C}(\tau)$ as a function of τ and T (both measured in units of $1/\lambda$). Large values correspond to lighter shades and the red dashed line is the contour to the value zero. (b) Time evolution of the concurrence in the absence of measurements (black solid line) and in the presence of measurements performed at time intervals: $T = 0.1\lambda$ (green dashed line), $T = 1\lambda$ (red dot-dashed line) and $T = 5\lambda$ (blue dotted line).

In the next section we will see that, for sufficiently short measurement time intervals T, such that $\langle\psi_0|\rho(T)|\psi_0\rangle \ll 1$, both quantum Zeno and anti-Zeno effects on the entanglement may occur.

3. Results

In the previous section, we have mentioned that the explicit analytical expression for the concurrence $\mathcal{C}^{(N)}(t)$ at time $t = NT$, i.e. after performing N measurements, becomes more complicated in the off-resonant case. In this section we compare the off-resonant entanglement dynamics in the absence and in the presence of measurements for two qubits initially in a maximal entangled state ($s = 0$), in both good and bad cavity limits. We note that, in general, the entanglement dynamics in the absence of measurements is strongly sensitive to the relative coupling parameter r_1 [2], while we will see that, in the presence of measurements, such dependence is often inhibited.

3.1. Bad-cavity limit: enhancement of the entanglement protection

We begin considering the bad-cavity limit, e.g. $R = \mathcal{R}/\lambda = 0.1$. In the off-resonant case here considered, and at short times, the dynamics of all initially entangled states does not depend strongly on r_1, so we consider the case $r_1 = r_2 = 1/\sqrt{2}$. For small values of the detuning $\delta < \mathcal{R}$ the behaviour of the concurrence in the presence of measurements does not change appreciably compared to the resonant case. Thus, the observed dynamics shows always the quantum Zeno effect for all values of T. We find a similar result in the dispersive regime, i.e. for values of the detuning $\delta \lesssim \lambda$.

In the subradiant scenario $\omega_1 = \omega_2$, increasing the detuning the anti-Zeno effect appears for values of T larger than a characteristic threshold value T^* that depends on the detuning, as shown in figure 1. In particular, for increasing values of the detuning, the Zeno region becomes smaller

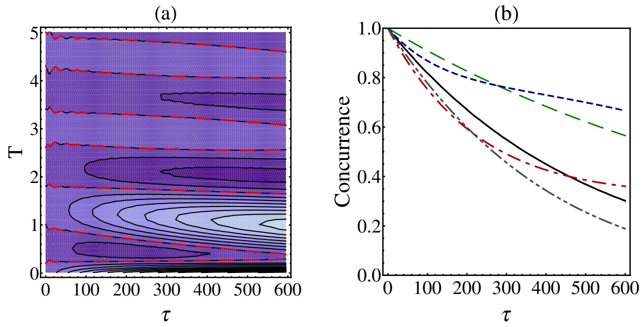

Figure 2. In the non-subradiant scenario ($\delta_1 = -\delta_2$) and bad cavity limit ($R = 0.1$), for $s = 0$, $\delta = 2$ and $r_1 = 1/\sqrt{2}$: (a) contour plot of $\mathcal{C}^{(N)}(\tau) - \mathcal{C}(\tau)$ as a function of τ and T (both measured in units of $1/\lambda$). Larger values correspond to lighter shades and the red dashed line is the contour to the value zero. (b) Time evolution of the concurrence in the absence of measurements (black solid line) and in the presence of measurements performed at time intervals: $T = 0.1\lambda$ (green dashed line), $T = 0.5\lambda$ (red dot-dashed line), $T = 1\lambda$ (blue dotted line) and $T = 2\lambda$ (gray dot-dot-dashed line).

and smaller, occurring only for very short measurement time intervals. A similar behaviour occurs when only one of the two qubits is coupled to the reservoir, that is, $r_1 = 0, 1$.

In the non-subradiant scenario $\omega_1 \neq \omega_2$, when the detuning is slightly larger than the reservoir width $\delta \gtrsim \lambda$, the dynamics presents new features. In more detail, for $\delta_1 = -\delta_2$, one can prove that the concurrence in the presence of measurements shows oscillations as a function of the measurement time interval T; thus quantum Zeno and anti-Zeno effects for the entanglement alternatively occur for increasing values of T, as shown in figure 2. Moreover, for $\delta \sim \lambda$, the quantum Zeno effect dominates again the dynamics for time intervals T of the order of the reservoir memory time. In this regime an interesting phenomenon happens, namely the quantum Zeno protection of entanglement is more efficient than in the resonant case, also for longer times.

3.2. *Good-cavity limit: monotone entanglement dynamics*

In the good cavity limit, e.g. for $R = \mathcal{R}/\lambda = 10$, the behaviour of the concurrence in the absence of measurements shows entanglement oscillations and revival phenomena due to the non-Markovian memory of the reservoir. Projective measurements performed on the qubits at time intervals T shorter than the reservoir memory time disentangle the qubits from the reservoir and destroy the entanglement oscillations and revival phenomena due to the system–reservoir correlations. In other words, as the measurements suppress more and more efficiently the feedback from the reservoir into the qubits, the shorter is T.

Thus, unlike the bad cavity case, in this regime the entanglement dynamics in the presence of measurements shows qualitatively similar behaviours for all values of the detuning as well as for both $r_1 = r_2 = 1/\sqrt{2}$ and $r_1 \neq r_2$. However, the Zeno and anti-Zeno regions still depend on r_j because the concurrence in the absence of measurements is strongly sensitive to the relative coupling parameter.

For values of the detuning $\delta < \mathcal{R}$, the system presents the quantum Zeno effect for all values of T, independently of the relative coupling r_j. In the dispersive regime $\delta > \mathcal{R}$, when both qubits are identically coupled to the reservoir ($r_1 = 1/\sqrt{2}$), the concurrence in the presence of measurements decreases monotonically to zero and the anti-Zeno effect occurs for values of T greater than a characteristic threshold value T^* that depends on the detuning, as shown in figure 3. For increasing values of the detuning the entanglement dynamics in the presence of measurements does not change appreciably: the amplitude of the oscillations decreases until it reaches the value obtained in the absence of measurements and the value of T^* decreases.

For $r_1 \neq 1/\sqrt{2}$, the entanglement dynamics in the presence of measurements starts to decrease approaching zero and then increases again towards its stationary value, which is zero only in the non-subradiant scenario. Although the concurrence shows always a qualitatively similar behaviour, the Zeno and anti-Zeno regions depend on the different detuning configurations, as one can understand by looking at the concurrence behaviour in the absence of measurements, see figure 4. Finally, we note that in the good cavity limit, the presence of the detuning enhances the appearance of the quantum anti-Zeno effect on the entanglement.

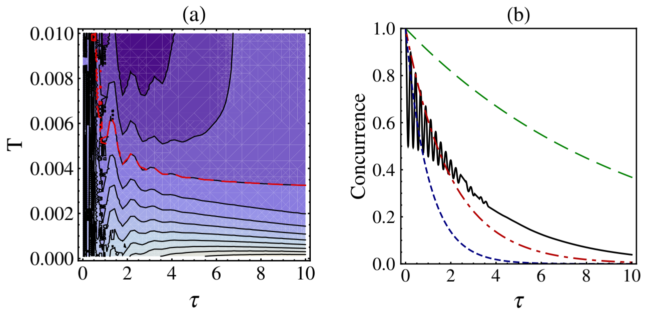

Figure 3. In the subradiant scenario ($\delta_1 = \delta_2$) and good cavity limit ($R = 10$), for $s = 0$, $\delta = 20$ and $r_1 = 1/\sqrt{2}$: (a) contour plot of $\mathcal{C}^{(N)}(\tau) - \mathcal{C}(\tau)$ as a function of τ and T (both measured in units of $1/\lambda$), where larger values are shown lighter and the red dashed line is the contour to the value zero. (b) Time evolution of the concurrence in the absence of measurements (black solid line) and in the presence of measurements performed at time intervals: $T = 0.001\lambda$ (green dashed line) and $T = 0.005\lambda$ (red dot-dashed line) and $T = 0.01\lambda$ (blue dotted line).

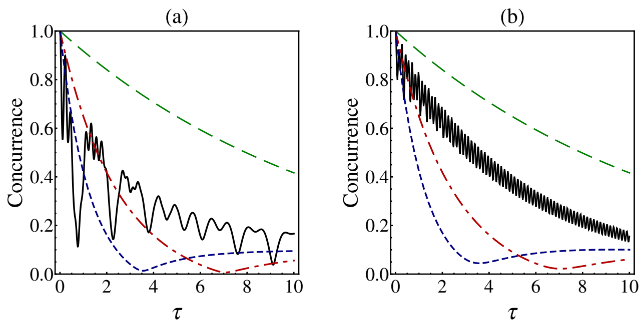

Figure 4. Time evolution of the concurrence in the good cavity limit ($R = 10$), for $s = 0$, $\delta = 20$ for $r_1 = 0.4$ in absence of measurements (black solid line) and in presence of measurements performed at time intervals: $T = 0.001\lambda$ (green dashed line), $T = 0.005\lambda$ (red dot-dashed line), $T = 0.01\lambda$ (blue dotted line). The two plots describe two different detuning configurations: (a) $\delta_1 = \delta_2 = 20\lambda$ and (b) $-\delta_1 = \delta_2 = 20\lambda$.

4. Summary

In this paper, we investigated the entanglement dynamics in the presence of measurements and looked at the conditions for the occurrence of both the quantum Zeno and the anti-Zeno effects on the entanglement. We found that the quantum Zeno effect always occurs when the measurement time interval T approaches zero, while for larger values of T, the quantum anti-Zeno effect may also occur. For certain values of the parameters, increasing values of T correspond to an alternative appearance of the Zeno and anti-Zeno effects.

In the bad cavity limit, both the behaviour of the concurrence in the presence of measurements and the Zeno and anti-Zeno regions are essentially independent of r_j. Finally, we note that when the measurement time interval is of the order of the reservoir memory time, the presence of the detuning enhances the protection of entanglement compared to the resonant case, so the entanglement can be more effectively protected for long times. On the contrary, in the good cavity limit the presence of the detuning enhances the appearance of the quantum anti-Zeno effect on the entanglement.

Acknowledgments

SM acknowledges financial support from the Turku Collegium of Science and Medicine, the Academy of Finland, the Magnus Ehrnrooth Foundation, the Turun yliopisto Foundation, the Väisälä Foundation and the Emil Aaltonen Foundation.

References

[1] Misra B and Sudarshan E C G 1977 *J. Math. Phys.* **18** 756
[2] Francica F, Maniscalco S, Piilo J, Plastina F and Suominen K-A 2009 *Phys. Rev.* A **79** 032310
[3] Maniscalco S, Francica F, Zaffino R L, Lo Gullo N and Plastina F 2008 *Phys. Rev. Lett.* **100** 090503
[4] Wootters W K 1998 *Phys. Rev. Lett.* **80** 2245
[5] Frerichs V and Schenzle A 1991 *Phys. Rev.* A **44** 1962
Schulman V L S 1998 *Phys. Rev.* A **57** 1509
[6] Itano W M, Heinzen D J, Bollinger J J and Wineland D J 1990 *Phys. Rev.* A **41** 2295
Fisher M C, Gutierrez-Medina B and Raizen M G 2001 *Phys. Rev. Lett.* **87** 040402
[7] Guthoöhrlein G R *et al* 2001 *Nature* **414** 49
Maunz P *et al* 2004 *Nature* **428** 50
[8] Sillanpää M A, Park J I and Simmonds R W 2007 *Nature* **449** 438
[9] Majer J *et al* 2007 *Nature* **449** 443
[10] Kofman A G and Kurizki G 2000 *Nature* **405** 546
Kofman A G and Kurizki G 1996 *Phys. Rev.* A **54** 3750
Facchi P, Nakazato H and Pascazio S 2001 *Phys. Rev. Lett.* **86** 2699
[11] Maniscalco S, Olivares S and Paris M G A 2007 *Phys. Rev.* A **75** 062119
Bellomo B, Lo Franco R and Compagno G 2007 *Phys. Rev. Lett.* **99** 160502